GRBV

V CONGRESSO NAZIONALE GRB 2022

RADIO DATA CHALLENGE THE BROADBAND MODELLING OF GRB160131A AFTERGLOW

Speaker

Dr. MARCO MARONGIU

Post-Doc Researcher
Osservatorio Astronomico di Cagliari
Sardinia - Italy

OAC

INAF
ISTITUTO NAZIONALE DI ASTROFISICA

COLLABORATORS : M. Marongiu (INAF - OAC), C. Guidorzi (University of Ferrara), G. Stratta (INAF – IAPS Roma), A. Gomboc (University of Nova Gorica - SI) , N. Jordana-Mitjans (University of Bath - UK), S. Dichiara (University of Maryland – USA), S. Kobayashi (ARI/LJMU – UK), D. Kopac (University of Ljubljana – SI), and C. G. Mundell (University of Bath - UK)

TRIESTE, Italy – 12th September 2022

Summary

Marongiu et al., 2022, A&A

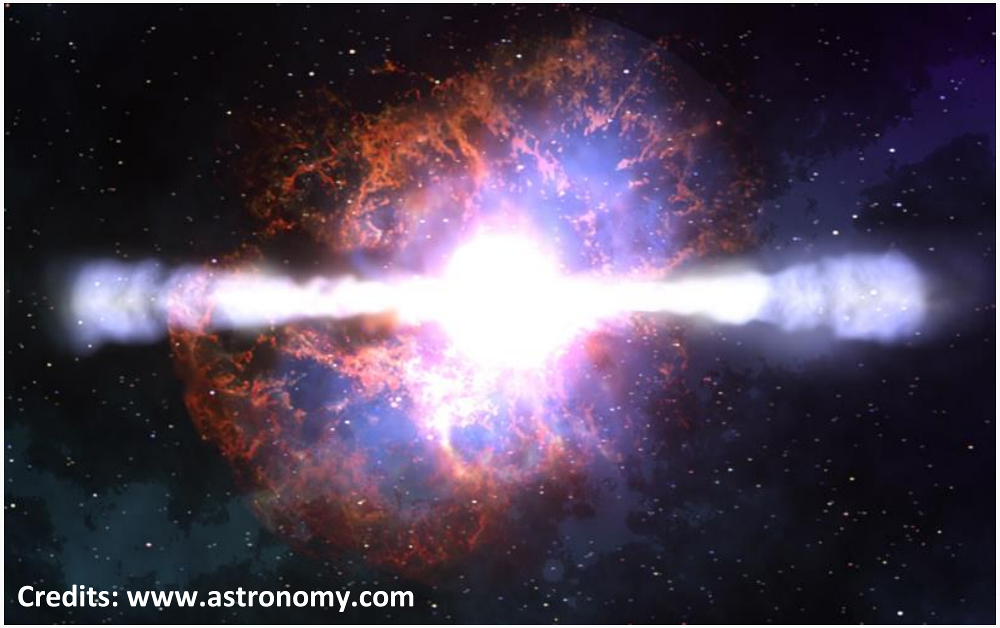

Broadband modelling of GRB160131A afterglow

↓

Rich, broadband, and accurate data set

- GRB Afterglows in a nutshell : why are they interesting to study?
- Broadband modelling of this GRB afterglow
- Discussion of our results

Identity card of GRB160131A

Marongiu et al., 2022, A&A

Discovered by Swift satellite
(Page & Barthelmy 2016)

$T_{90} \sim 330$ s (Cummings et al. 2016) → Long-GRB

z = 0.972 (Malesani et al. 2016; de Ugarte Postigo et al. 2016)

$E_{\gamma,iso} = 8.3 \cdot 10^{53}$ erg (Tsvetkova et al. 2016)

Broadband data from:

- VLA (radio band)
- Optical telescopes
- Swift UVOT and XRT (UV and X-ray)

Why do we study GRB afterglows?

Relevant contributions

- Physics of the prompt emission
- Shock microphysics
- Jet properties

Relevant contributions in RADIO

- Reverse shock
- Nature of progenitors of GRBs

The radio frequencies are very important, but GRB radio afterglows are faint sources!

Radio detection rate of GRB afterglows is only 30%

More phenomena, more complexities!

Physical phenomena correlated

- Sy
- Compton
- Jet properties
- Energy injection
- Optical extintion
- Radio scintillation

The richness of the data set collected for GRB160131A makes it an ideal test bed for the standard GRB afterglow model

…and modelling: more complete physical information about GRB afterglows!

Modelling approaches

Empirical approach

We modelled SEDs and light curves with simple empirical functions (single power-law, broken power-law, and double broken power-law)

Constraint of the behaviour of the GRB afterglow emission, in terms of the main observational features (breaking frequencies and possible jet break time) and the kind of CMB (ISM-like vs. wind-like).

Modelling approaches

Physical approach

Marongiu & Guidorzi, 2021

We modelled the data set of the GRB afterglow emission through a Python code called sAGa (Software for AfterGlow Analysis)

Parameter	Unit	Description
p	–	Power-law index of the electron energy distribution
ϵ_e	–	Fraction of the blastwave energy delivered to relativistic electrons
ϵ_B	–	Fraction of the blastwave energy delivered to magnetic fields
$E_{K,\mathrm{iso},52}$	10^{52} erg	Kinetic energy of the explosion (in units of 10^{52} erg)
n_0	cm^{-3}	Density for ISM-like CBM
A_*	5×10^{11} g cm^{-1}	Parameter connected with the wind-like density CBM
A_V	mag	Extinction in the host galaxy
t_j	d	Jet break time
$t_{ei,1}$	d	Start time of the first injection
$t_{ei,2}$	d	Start time of the second injection
m	–	Injection index
m_2	–	Injection index (in case of two bumps during the energy injection regime)

Modelling strategy

Synchrotron: forward shock
(Granot & Sari 2002, and the references therein)

Inverse Compton
(Sari & Esin 2001; Piran 2004; Zhang et al. 2007; Laskar et al. 2014, Granot & Sari 2002)

Jet properties (uniform)
- ✓ pure edge effect (e.g. Panaitescu et al. 1998; Granot 2007)
- ✓ sideways expansion effect (e.g. Rhoads 1999; Sari et al. 1999)

Energy injection
(Zhang & Mészáros 2002; Granot & Kumar 2006; Gao et al. 2013; Nousek et al. 2006; Liang et al. 2007; Margutti et al. 2010; Hascoët et al. 2012)

Non-relativistic/Newtonian ejecta
(Wijers et al. 1997; Zhang 2019; Waxman 1997; Chevalier & Li 2000; Livio & Waxman 2000; Zhang & MacFadyen 2009; Frail et al. 2000; van Eerten et al. 2010; Leventis et al. 2012)

Dust extinction in the host galaxy along the sightline
(Pei 1992)

Interstellar scintillation effect
(Rickett 1990; Goodman 1997; Walker 1998; Frail et al. 1997, 2000; Goodman & Narayan 2006; Granot & van der Horst 2014; Misra et al. 2021; Laskar et al. 2014)

UV absorption by neutral hydrogen (from z > 1)
(Madau 1995)

Photoelectric absorption for X-ray data
(Morrison & McCammon 1983)

Optical/X-ray data

Temporal index -1.25:
Forward shock

Temporal index -1:
Energy injection

Temporal index -1.8:
Jetted emission

1. ISM-like CBM
2. The transition between fast and slow cooling regime is not constrained by optical/X-ray observations
3. p = 2.2
4. Both ν_c and ν_m lie below optical frequencies $\nu_{opt} = 3 \times 10^{14}$ Hz already at 10^{-3} d
5. A milder jet break model (pure edge effect) is in accordance with the optical/X-ray data

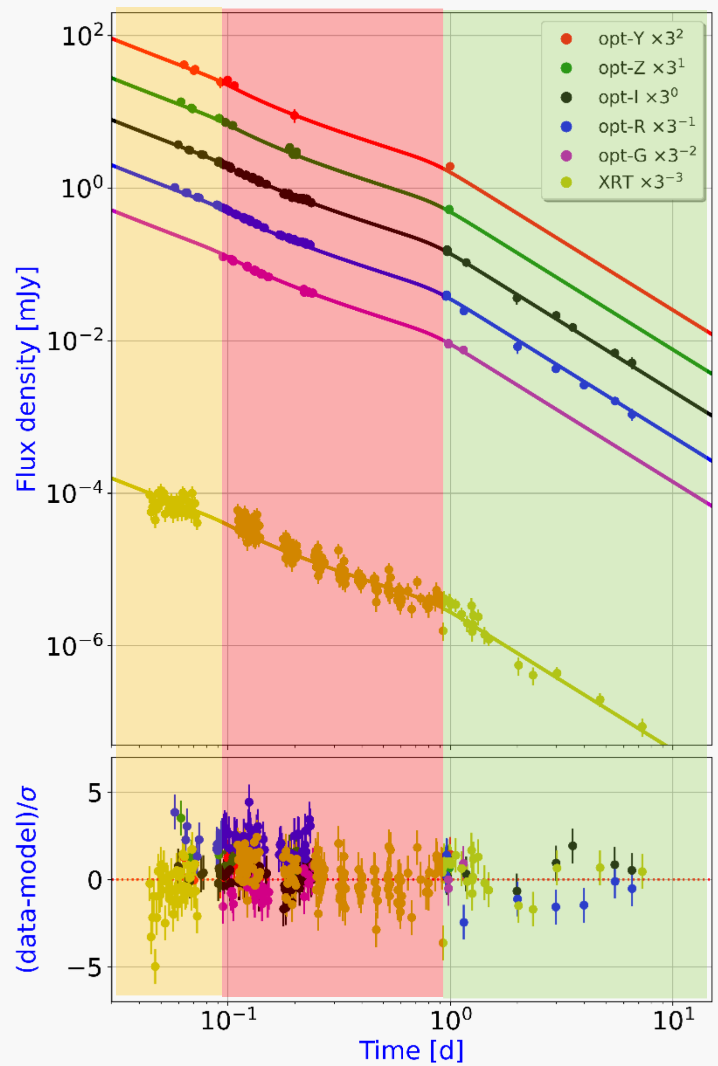

Empirical model: double broken power-law

VLA radio data - SEDs

G. Jansky Very Large Array (VLA)
Frequencies : 5-40 GHz
Epochs : 0.8-150 d

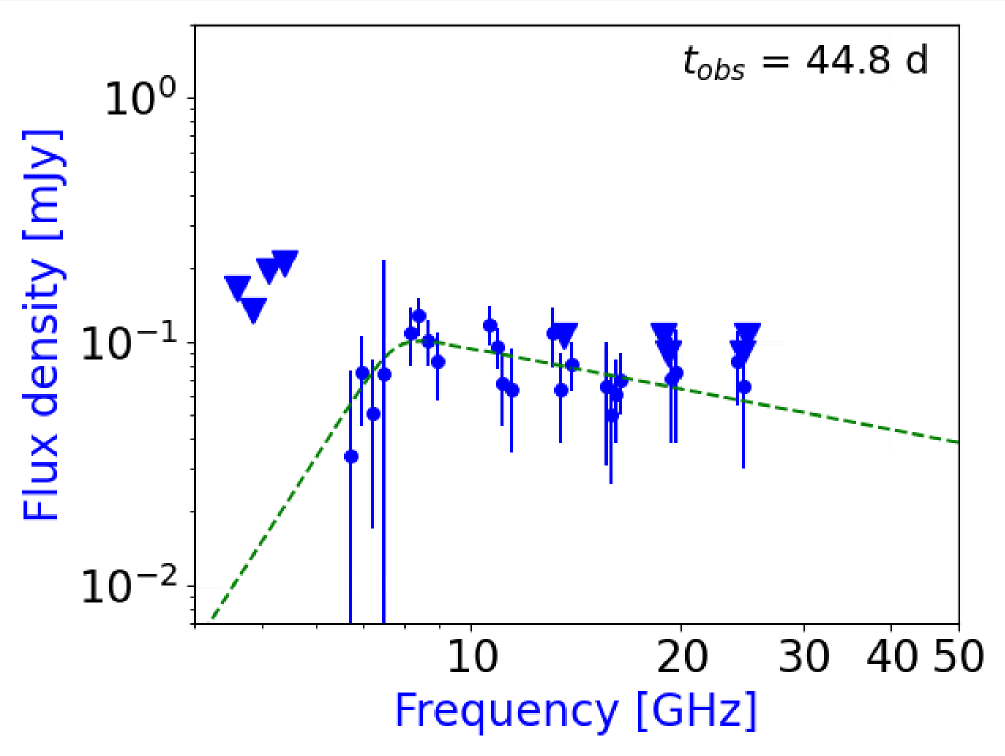

Ignore peaks
Compare the resulting spectral indices with those expected from the synchrotron emission of GRB afterglows

1. The slow-cooling regime occurs at times less than 0.8 d
2. At 12.7 d the self-absorption frequency is about 7 GHz

VLA radio data - SEDs

G. Jansky Very Large Array (VLA)
Frequencies : 5-40 GHz
Epochs : 0.8-150 d

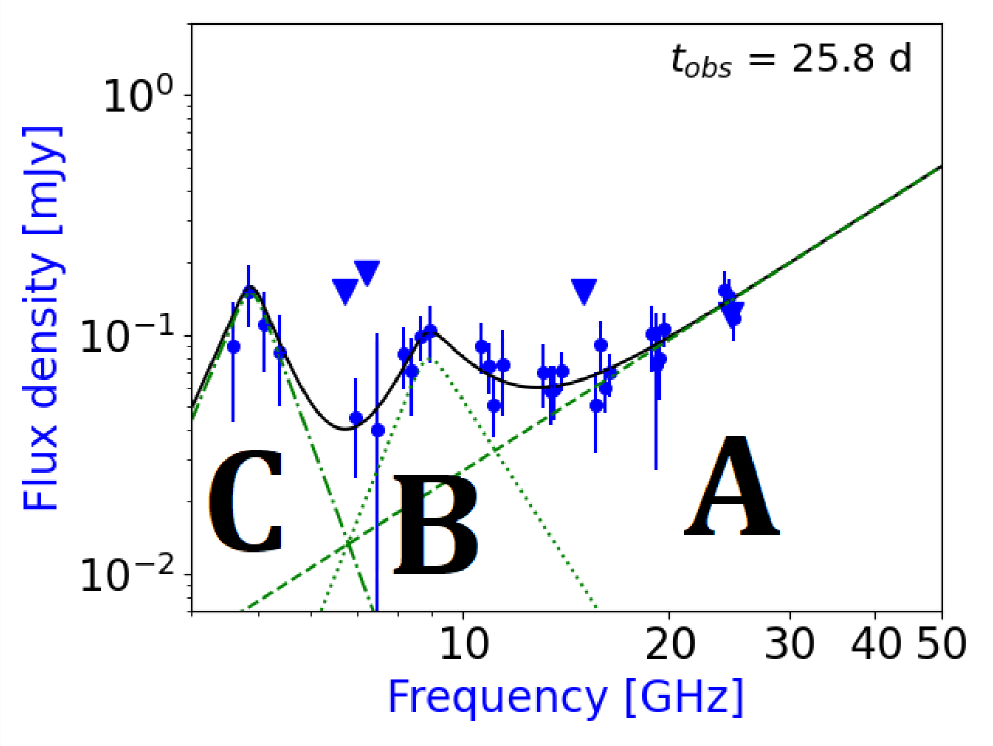

Consider peaks
Multi-component approach

The radio data set is composed of three spectral components
"A" is connected with the continuum associated with FS emission

VLA radio data - Light-curves

G. Jansky Very Large Array (VLA)
Frequencies : 5-40 GHz
Epochs : 0.8-150 d

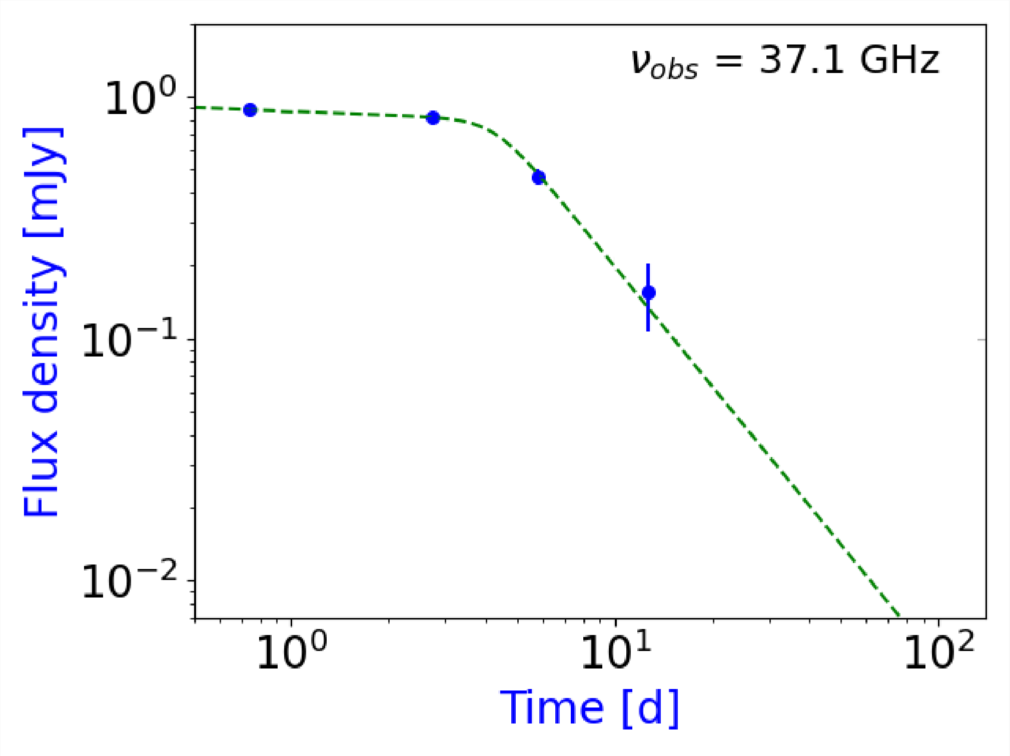

Radio light-curves help to constrain the jet opening angle

1. The passage of ν_m occurs at $t \lesssim 3$ d in the 8 – 26 GHz light curves
2. The passage of ν_c occurs after 45 d in the 8 – 14 GHz light curves
3. The passage of ν_c occurs at $t \sim 120$ d in the 14 – 26 GHz light curves

Modelling with sAGa

Iterative analysis

Starting points

$$\mathbf{p = 2.2}$$
$$\boldsymbol{\varepsilon_B = 0.01}$$
$$\boldsymbol{\varepsilon_e \sim 0.1}$$
$$\mathbf{n_0 = 1\ cm^{-3}}$$
$$\mathbf{E_{k,iso,52} = 50}$$
$$\mathbf{A_V = 0.1}$$
$$\mathbf{t_j = 1\ d}$$
$$\mathbf{m = 0.2}$$

Modelling with sAGa

From optical to X-rays

Parameter	Unit	UVOIR/X-ray
p	–	$2.14^{+0.02}_{-0.01}$
ϵ_e	–	$(1.3^{+0.3}_{-0.2}) \times 10^{-2}$
ϵ_B	–	$(9.3^{+9.0}_{-5.1}) \times 10^{-2}$
n_0	cm^{-3}	$10.7^{+12.8}_{-6.4}$
E_{52}	10^{52} erg	$(4.9^{+0.9}_{-0.8}) \times 10$
A_v	mag	$(1.8 \pm 0.4) \times 10^{-1}$
t_j	d	$0.82^{+0.03}_{-0.02}$
θ_j	deg	$5.6^{+0.6}_{-0.7}$
t_{NR}	d	$(2.7^{+1.1}_{-0.7}) \times 10^{2}$
$t_{b,0}$	d	$(2.09 \pm 0.01) \times 10^{-1}$
m	–	0.120 ± 0.002
ν_m $^{(b)}$	Hz	3.0×10^{11}
ν_c $^{(b)}$	Hz	3.1×10^{12}
ν_{sa} $^{(b)}$	Hz	3.4×10^{11}
ν_{ac} $^{(b)}$	Hz	2.3×10^{12}
$t_{trans,51}$	d	1.8×10^{-2}
$t_{trans,12}$	d	0.5
χ^2_r	–	0.97

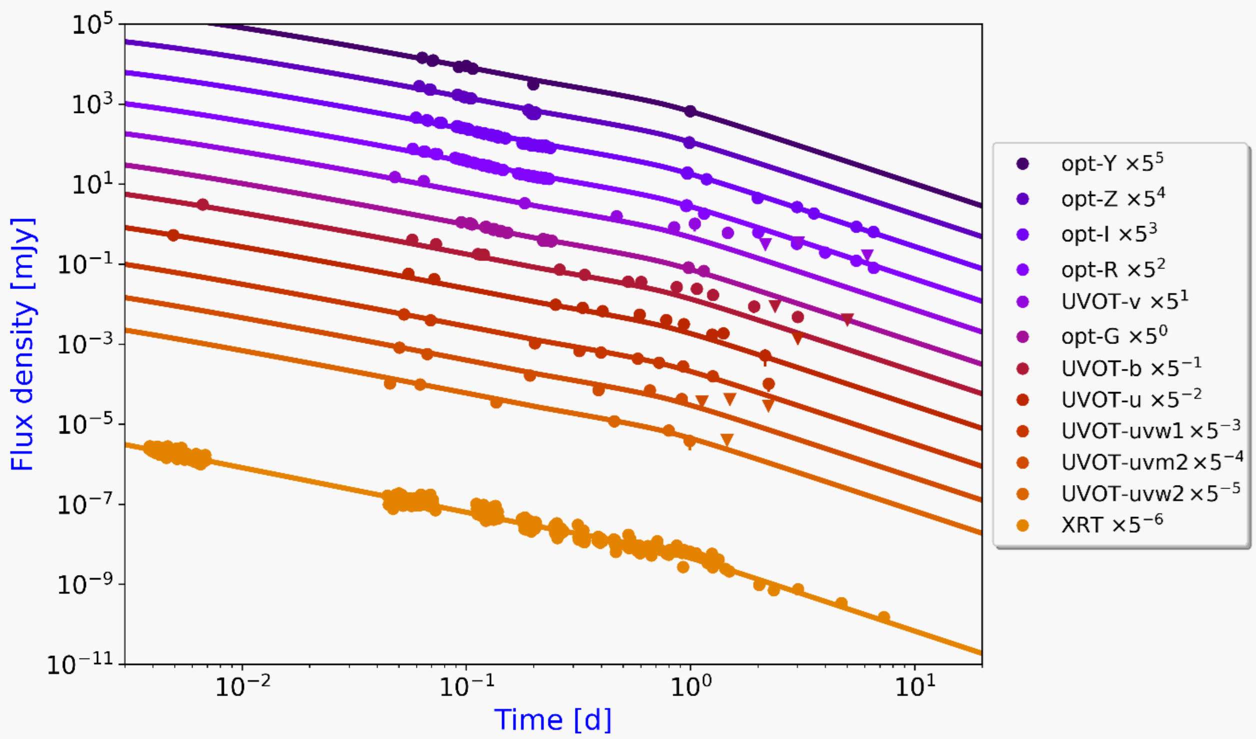

Modelling with sAGa

From radio to X-rays

Parameter	Unit	Radio/X
p	–	2.20 [a]
ϵ_e	–	$(3.4^{+0.5}_{-0.2}) \times 10^{-2}$
ϵ_B	–	$(1.5 \pm 0.3) \times 10^{-3}$
n_0	cm^{-3}	$(3.6^{+2.7}_{-0.8}) \times 10^{1}$
E_{52}	10^{52} erg	$(1.2^{+0.1}_{-0.2}) \times 10$
A_v	mag	0.2 ± 0.1
t_j	d	0.9 ± 0.1
θ_j	deg	$7.7^{+0.7}_{-0.3}$
t_{NR}	d	$(1.2^{+0.1}_{-0.3}) \times 10^{2}$
$t_{b,0}$	d	$(2.10^{+0.01}_{-0.03}) \times 10^{-1}$
m	–	$(5.03^{+0.05}_{-0.02}) \times 10^{-2}$
ν_m [b]	Hz	1.7×10^{11}
ν_c [b]	Hz	5.9×10^{14}
ν_{sa} [b]	Hz	1.5×10^{11}
ν_{ac} [b]	Hz	2.9×10^{12}
$t_{trans,51}$	d	9.2×10^{-5}
$t_{trans,12}$	d	1.3
χ_r^2	–	10.97

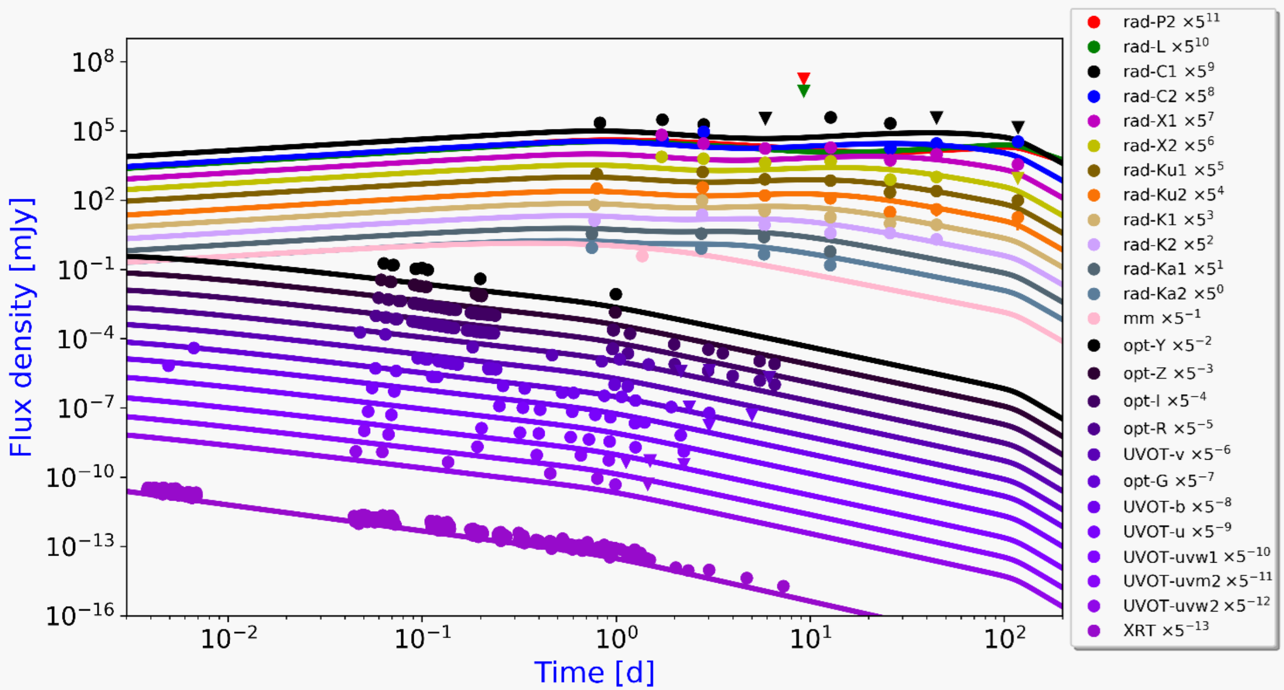

Problematic features at radio frequencies

Possible assumptions for the afterglow of GRB160131A

Time varying shock micro-physics parameters, as suggested for the afterglow emission from GRB190114C (Misra et al., 2021)

The transition from different CBM a wind-like to ISM-like CBM as in the case of the afterglow of GRB140423A (Li et al., 2020)

Another jet model, in light of the evidence of other jet models used to interpret the broadband data for several GRB afterglows (two-component, structured, or other more complex regimes) (e.g. Kangas et al., 2021)

Energy injection

Re-brightening of the GRB afterglow connected with the injection from the central engine of ejecta into the blastwave shock

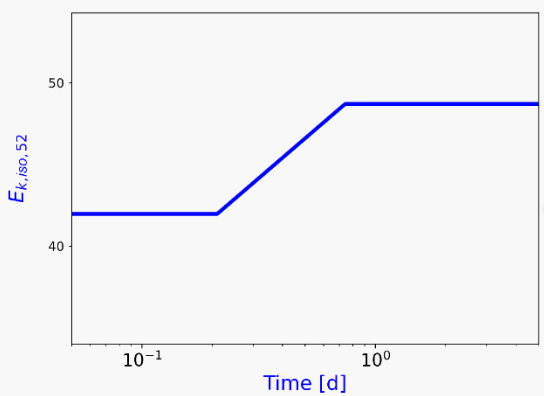

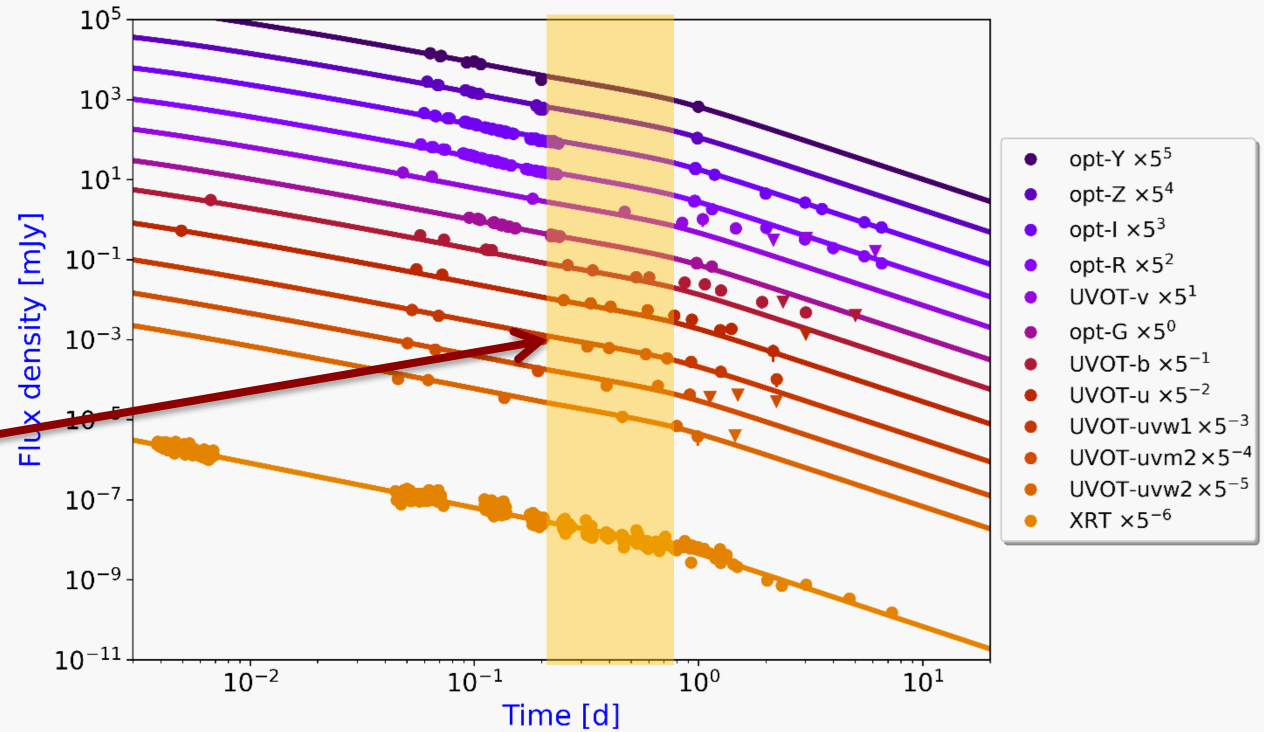

Energy injection

The pronounced optical flattening could be interpreted as:

- Change of the CBM (Gendre et al. 2010)
- Reverse shock (Gendre et al. 2010)
- Two-component jet (Kann et al. 2018)

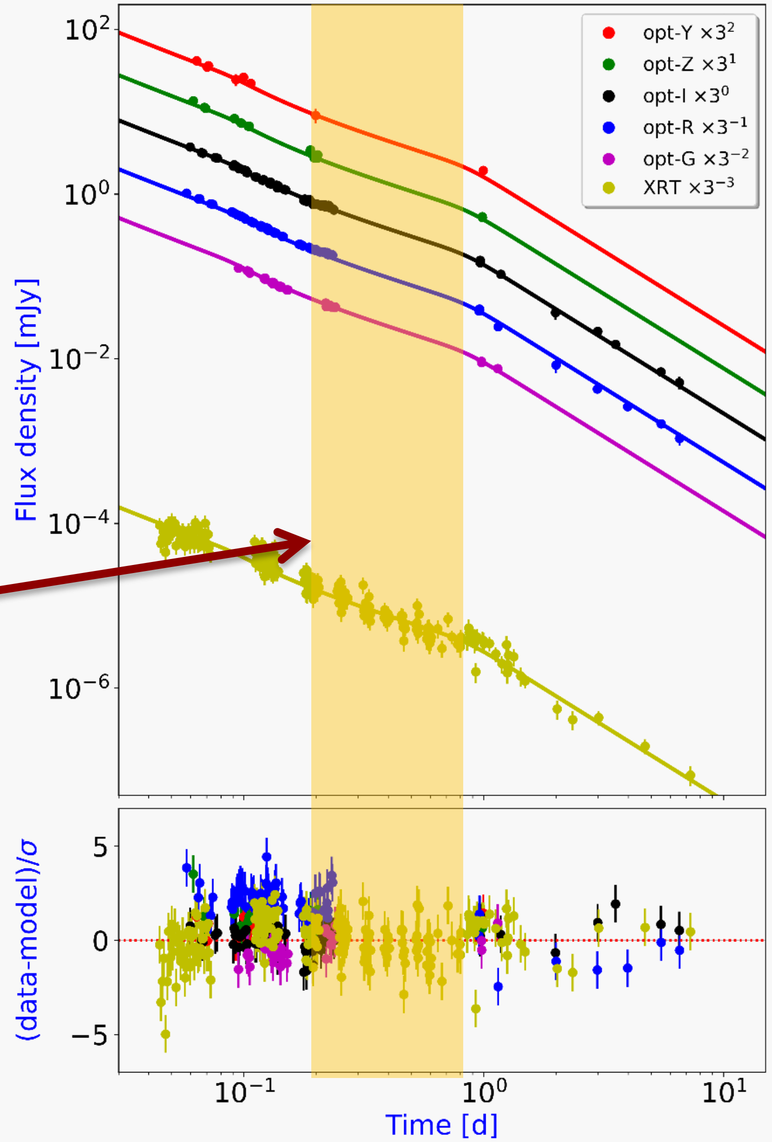

Insterstellar scintillation effects

The presence of peaks in radio SEDs had already been observed in other sources, and the main candidate to explain this pronounced radio variability is the ISS
(e.g. Horesh et al. 2015)

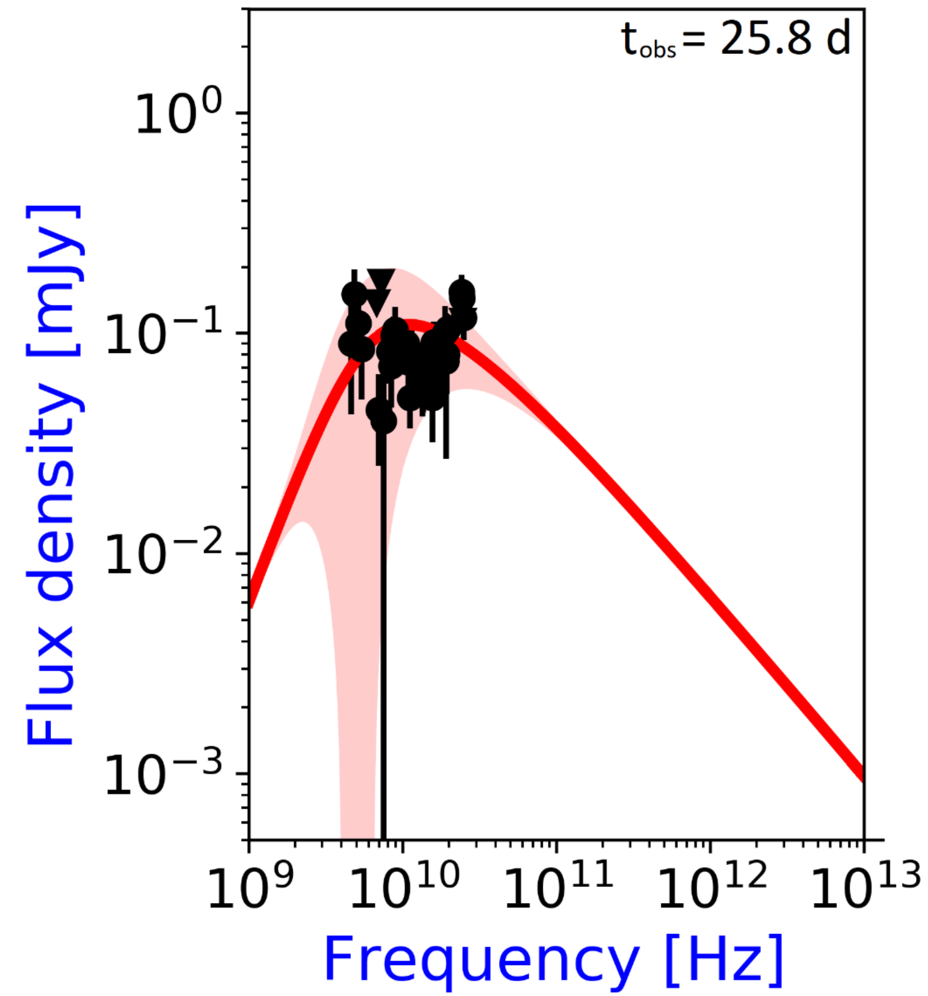

Reverse shock

Excluded…why?

1. **Theoretical prescriptions taken up by the RS literature** (e.g. Laskar et al. 2018)

2. **The typical peaks connected with RS emission are much broader ($\Delta\nu/\nu \sim 3$) than what we find ($\Delta\nu/\nu \sim 0.5$)**

3. **The CBM density typically associated with the broadband detections of RS emission ($n_0 \lesssim 10^{-2}\ \mathrm{cm}^{-3}$) is lower than our lower limit estimated with sAGa ($n_0 \gtrsim 5\ \mathrm{cm}^{-3}$)**

Take-home messages

- The inclusion of radio data in the broadband set of GRB160131A makes a self-consistent modelling barely attainable within the standard model of GRB afterglows
- Radio frequencies are crucial to better constrain the spectral slope of the GRB afterglow emission
- We need more complete models, data and facilities to explain the broadband emission from GRB afterglows

Thank you for your attention!

Marco Marongiu – Post-Doc Researcher
INAF/OAC – Cagliari Astronomical Observatory

E-mail: **marco.marongiu@inaf.it**